Nucleic Acids Research, 2025, **53**, gkaf232
https://doi.org/10.1093/nar/gkaf232
Molecular and Structural Biology

Small nucleolar RNAs promote the restoration of muscle differentiation defects in cells from myotonic dystrophy type 1

Baptiste Bogard[1,2], Hélène Bonnet[1], Ekaterina Boyarchuk[1], Gilles Tellier[1], Denis Furling[3], Vincent Mouly[3], Claire Francastel[1,4], Florent Hubé[1,4,*]

[1]Université de Paris Cité, CNRS, UMR7216 Épigénétique et Destin Cellulaire, F-75013 Paris, France
[2]Present Address: UMEÅ University, Department of Molecular Biology, 901 87 Umeå, Sweden
[3]Sorbonne Université, Inserm, Association Institut de myologie, Centre de recherche en myologie, UMRS 974, 47 boulevard de l'Hôpital, 75013 Paris, France
[4]Sorbonne Université, CNRS UMR7622, Inserm U1156, Institut de Biologie Paris Seine, Laboratoire de Biologie du Développement, 75005 Paris, France
[*]To whom correspondence should be addressed. Email: florent.hube@cnrs.fr

Abstract

Recently, the repertoire of human small nucleolar noncoding RNAs (snoRNAs) and their potential functions has expanded with the discovery of new snoRNAs and messenger RNA (mRNA) targets, for which snoRNA-guided modifications may influence their stability, translatability, and splicing. We previously identified snoRNAs that are abundant in healthy human muscle progenitor cells. In this study, we demonstrated that SNORA40 and SNORA70 loss-of-function impairs myogenic differentiation. Interestingly, gain-of-function can rescue impaired differentiation muscle progenitor cells in myotonic dystrophy type 1 (DM1). We identified cyclin D3 (CCND3) mRNA, which is partially located in the nucleolus, as a target for SNORA40 and SNORA70, which are required for its pseudouridylated status. Expression of the CCND3 protein is required for muscle progenitors to exit the cell-cycle when they are induced to differentiate. We revealed that this switch requires SNORA40/70. Finally, we observed that DM1 cells show reduced levels of SNORA40/70 and undetectable CCND3 protein. However, restoring normal levels of SNORA40/70 partially restored CCND3 protein expression, coinciding with improved cell fusion capacity in DM1 muscle progenitors. Collectively, these data suggest that this effect may stem from SNORA40/70-dependent pseudouridylation of CCND3 mRNA, emphasizing snoRNAs as key players in normal and pathological muscle differentiation.

Graphical abstract

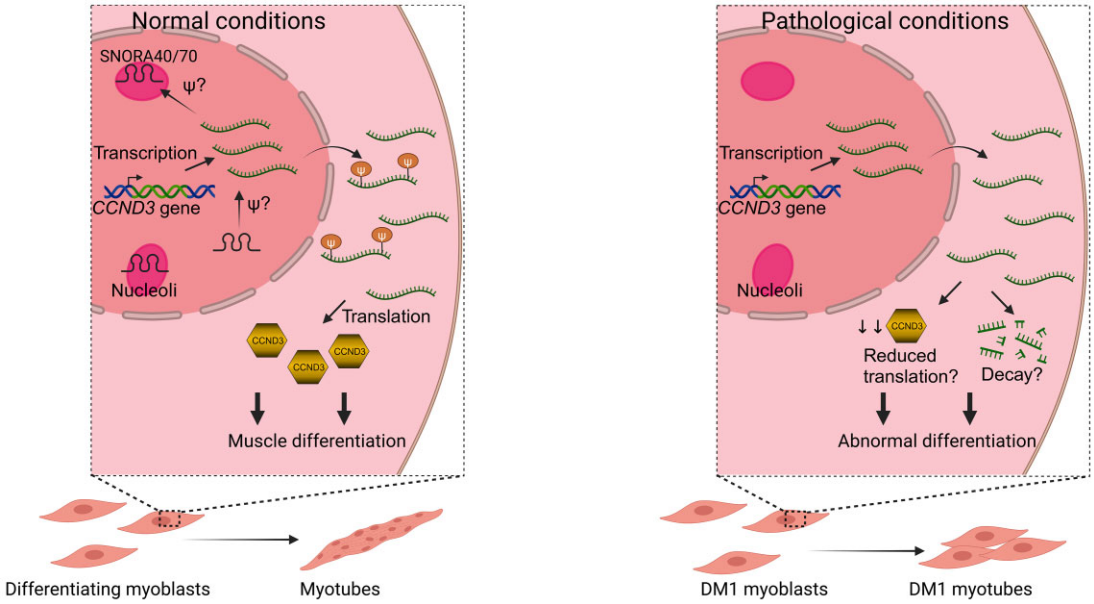

Received: July 15, 2024. **Revised:** February 19, 2025. **Editorial Decision:** March 7, 2025. **Accepted:** March 12, 2025

Introduction

Myotonic dystrophy type 1 (DM1) is an autosomal dominant disorder and the most common form of adult-onset muscular dystrophy, with an incidence of 1 in 8000 births worldwide (OMIM 160900). Neuromuscular disease is caused by a CTG expansion in the 3′-untranslated region (UTR) of the differentiation medium (DM) protein kinase gene [1]. Mutant transcripts containing expanded repeats are retained in nuclear aggregates that sequester MBNL1 splicing factors. They alter the activity of other RNA binding proteins, leading to alterations in RNA metabolism, including inappropriate regulation of alternative splicing (AS) events [2, 3]. Splicing dysregulation of a subset of pre-mRNAs, including the cardiac troponin T, chloride voltage-gated channel 1, and troponin T2 transcripts, is the major trans-dominant effect that causes disease symptoms, such as muscle wasting, myotonia, and cardiac conduction defects (see for review [4]). In addition, myogenesis, the process by which precursor myoblasts (MB) exit the cell-cycle to fuse into multinucleated myotubes (MT) and then muscle fibers, is altered, which disrupts the expression of muscle regulatory factors (MRFs) (see for review [5]), and other proteins involved in the differentiation process [6]. For example, the myogenic factor MEF2A is abnormally upregulated in the disease [6]. In addition, the cyclin D3 (CCND3) protein plays a special role as a regulator of cell-cycle exit and promoter of myotube formation [7, 8]. Little is known about the involvement of CCND3 in these processes, but CCND3 may interact with and inhibit the activity of the cyclin-dependent kinase 2 protein *in vitro* [9]. Furthermore, an *in vivo* study demonstrated that CCND3 co-localizes in the nucleus with the MRFs myogenin and p21, whose expression levels gradually increase during the early stages of skeletal muscle satellite cell differentiation [10]. Interestingly, the CCND3 pathway appears to be reduced in DM1 muscle cells [11].

Small nucleolar RNAs (snoRNAs) are a class of small noncoding RNAs (sncRNAs), most of which are located within the introns of protein-coding and noncoding genes in mammals. Their production relies on the transcription of the host gene, followed by splicing and debranching of the intron to be processed into mature snoRNAs.

They are localized to the nucleolus, where they mainly act as guides for posttranscriptional RNA modification through base-pairing with their target RNA molecule [11]. They are classified based on structural features and sequence motifs, known as the C/D- and H/ACA box, and define two subgroups. C/D (SNORD) and H/ACA (SNORA) snoRNAs each recruit a different constitutive set of four core proteins to form classical ribonucleoprotein (RNP) particles. Their canonical function is to guide the nonautonomous enzymes, fibrillarin and dyskerin, to catalyze site-specific 2′-O-methylation and pseudouridylation (Ψ), respectively, on ribosomal RNAs (rRNAs), which is important for ribosome biogenesis and translation accuracy [12–14]. However, recent studies suggest that mRNAs are also targets of snoRNA-guided RNA modifications that affect their stability, translatability, or splicing ([15]; see for review [16]). Furthermore, the expression of snoRNAs was dysregulated in human diseases, such as cancer (e.g. acute myeloid leukemia ([17] and colorectal cancer [18]), or congenital heart defects [19]. In addition, few dysregulated snoRNAs act as oncogenes or tumor suppressors and participate in disease progression, such as SNORA42, which is upregulated in nonsmall cell lung cancer and promotes cell proliferation and colony formation [20].

Although aberrant splicing of mRNAs is a major contributor to DM1 disease, this "splicing disease" may have a broader effect than just affecting protein production. We previously reported the splicing-dependent expression of over 50 short intron-derived, noncoding RNAs (SIDs), which are associated with the muscle differentiation of human MB [19]. This fine regulation through the AS of introns may be impaired in cells from DM1 patients [19].

To identify novel sncRNAs on a large scale, without a priori knowledge of their sequence or location in the genome, we implemented an unbiased medium RNA sequencing (RNA-seq) on size-fractionated RNAs (>50 and <200 nt) [21]. We examined two families of snoRNAs, namely SNORA40 and SNORA70, which were abundant in healthy muscle progenitors. We found that their levels were markedly reduced in muscle progenitors from DM1 cells. Restoring normal levels of SNORA40 or SNORA70 rescued the differentiation defects that characterize muscle cells from DM1 patients. This occurs through an increase in the expression of CCND3 protein, which is required for muscle progenitors to undergo myogenic differentiation. We showed that CCND3 mRNA is partially located in the nucleolus, co-precipitates with SNORA40 and SNORA70, and is pseudouridylated. Therefore, the CCND3 mRNA is likely a new target for pseudouridylation by SNORA40 and SNORA70, which in turn may increase its translatability.

Materials and methods

Bioinformatics analysis

Total RNA-seq data were analyzed using RASflow_EDC v0.7.7 (https://github.com/parisepigenetics/RASflow_EDC, adapted from RASflow [22]) with HISAT2 [23] alignment software on the hg38 genome and featureCounts (with -M -O options; [24]) for annotation using Gencode v41. The complete list of parameters and tool versions is available upon request. The workflow was run on the HPC cluster of iPOP-UP, hosted by RPBS and funded by the Université Paris Cité (IDEX).

Medium RNA-seq was analyzed using Bowtie2 version 2.3.4.1, Bedtools v2.27.1, and Samtools 1.9. The complete list of parameters used was set to default.

Plasmid constructs

All plasmids used in this study are presented in Supplementary Fig. S1. Briefly, a 1876-nt fragment containing the CMV promoter, prepared from a split enhanced green fluorescent protein (eGFP) sequence, in which a chimeric intron with the sequence for SNORA40 (NR_002973.1) was inserted, and a polyA signal was synthesized (Eurofins Scientific SE, Luxembourg). The fragment was then subcloned into pcDNA3 (Thermo Fisher Scientific, Waltham, USA) and used as a template to generate all the other constructs (Addgene #200644, #200645, and #200646) by replacing the SNORA40 sequence with the reference sequence of SNORA70 (NR_000011) or with the following random sequence: 5′-TTTTAGTTCTGATGAGGTACTTAGACGG GAGT-TCTTAAGCATTGCGCCGTCTAGTCCGGGGCC CAAAAGTACCATATGTACA-3′ (Eurofins Scientific SE, Luxembourg).

Antibodies

Primary antibodies were directed against α-tubulin (sc32293, Santa Cruz Biotechnology Inc., Dallas, USA), cyclin D3 (26755-1-AP, Proteintech Group Inc., Rosemont, USA), α-tubulin (11224-1-AP, Proteintech), pseudouridine (c15200236, Diagenode, France), and Xpress-tag (sc499, Santa Cruz Biotechnology Inc.). Donkey anti-rabbit or anti-mouse secondary antibodies coupled with the horseradish peroxidase (AP187P and AP192P, respectively, Sigma–Aldrich, Saint-Louis, USA) were used for western blot analysis. Donkey anti-mouse secondary antibodies conjugated with Alexa Fluor 488 or Alexa Fluor 594 (Jackson ImmunoResearch Laboratories Inc., Philadelphia, USA) were used for immunofluorescence.

Cell culture

We used human immortalized MB (LHCN-M2, MB) derived from the pectoralis major muscle of a 41-year-old male and their *in vitro* differentiated counterpart myotube (MT) cell lines [21, 25] (provided by V. Mouly, MyoLine Platform, Myology Institute, Paris, France), and a cell line (DM1 MB) obtained from the gastrocnemius muscle of an 11-year-old female patient with DM1 disease (1300 CTG in blood), which was provided by Denis Furling (MyoLine platform, Myology Institute) [25]. We used cells from passages 5 to 20 maximum. Briefly, cells were cultured at 37°C in growth medium (GM) consisting of DMEM/F12, GlutaMAX™ (Thermo Fisher Scientific, Waltham, USA) supplemented with 20% fetal bovine serum (Dominique Dutscher SAS, France), 100 U/ml penicillin, and 100 µg/ml streptomycin (all from Sigma–Aldrich). *In vitro* differentiation was induced for 7 days by replacing the GM with the DM (DM = GM without 20% fetal bovine serum). Primary MB from three healthy controls and three patients with congenital DM1 (>1000 CTG) were cultured at 37°C on dishes pre-coated with 2% gelatin in GM supplemented with 0.5 ng/ml basic fibroblast growth factor (Merck Millipore, France), 5 ng/ml human epidermal growth factor (Sigma–Aldrich), 5 ng/ml insulin (Sigma–Aldrich), 50 µg/ml fetuin (Sigma–Aldrich), and 0.2 µg/ml dexamethasone (Sigma–Aldrich).

RNA isolation

Total RNA was isolated using Tri Reagent® (Sigma–Aldrich) according to the manufacturer's instructions as previously described [25]. Before detection of snoRNAs by reverse transcription-polymerase chain reaction (RT-PCR) or northern blotting, short and long RNAs were purified using Nucleospin® microRNA (miRNA) (Macherey-Nagel GmBH & Co. Germany) according to the manufacturer's instructions and as previously described [25].

qRT-PCR

RNA was isolated as described above and reverse-transcribed into complementary DNA (cDNA) as previously described [25, 26]. The primers used for amplification are listed in Supplementary Table S1. Quantitative PCR was done using the SensiFAST™ SYBR® No-ROX Kit (Bio Technofix, France) with the LightCycler 480 real-time PCR system (Roche, Switzerland). Each quantitative real-time reverse-transcription PCR (qRT-PCR) was performed on RNA isolated from independent cell cultures (biological replicates; $n \geq 4$), and each RNA sample was included as a duplicate (technical replicates) on the PCR plate, including a no-template negative control. The relative expression of genes was calculated using the comparative C_T method [25, 26], i.e. 2[(Mock sample − Mock control) − (Target sample − Target control)]. Statistical analysis was performed using a two-way ANOVA Tukey's multiple comparisons test in GraphPad Prism 9 software.

Protein extraction and western blot analysis

Cells were lysed using RIPA buffer [150 mM NaCl, 0.5% sodium deoxycholate, 0.1% SDS, 50 mM Tris−HCl (pH 8), 1% NP-40] and protein concentration was measured using the Bradford assay (Sigma–Aldrich). Equal amounts of proteins were analyzed by sodium dodecyl sulfate–polyacrylamide gel electrophoresis and immunoblotting as described previously [25, 27].

Transfection of antisense oligonucleotide gapmers

The antisense oligonucleotide (ASO) used to knock down SNORA40 and SNORA70 were 5-10-5 RNA/DNA/RNA chimeric oligonucleotides linked through a phosphorothioate backbone consisting of 10 deoxyribonucleotides flanked by five 2′ O-methyl ribonucleotides at both ends [28]. Not all ASOs suppressed SNORA expression levels with the same efficiency because of their position on the snoRNA sequence (hindrance of the 3D structure, competition with RNP proteins, etc.); therefore, we used several ASOs to increase the knockdown efficiency (Supplementary Fig. S2) and reduce off-target effects as observed with small interfering RNAs [29]. The sequences of the ASOs are listed in Supplementary Table S1. MB were plated at 250 000 cells per well in a six-well plate. After 24 h, the cells were transfected with 50 nM of ASOs using Lipofectamine RNAiMAX transfection reagent (Thermo Fisher Scientific). Blocking ASOs, constituted of RNA nucleosides only, were transfected as mentioned earlier (Supplementary Table S1).

Electroporation of plasmids

Electroporation of plasmids was done using the SF Cell Line 4D-Nucleofector™ kit and the 4D-Nucleofector X Unit (Lonza, Switzerland) based on the manufacturer's instructions. Briefly, 10^6 cells per condition were resuspended in 100 µl of electroporation buffer and transferred into a Nucleocuvette™ vessel (Lonza). Then, 5 µg of plasmid was added and the cells were electroporated using the pulse code CA168. Finally, 500 µl of pre-warmed GM was added, to the Nucleocuvette™ vessel, and the electroporated cells were seeded into a six-well plate.

Calculation of the fusion index

Electroporated or transfected cells were grown on coverslips coated with 0.1% gelatin in GM. After 24 h, GM was replaced with DM to induce normal and DM1 myoblast differentiation for 5 days. Immunofluorescence experiments were performed as previously described [30] using a monoclonal anti-α-tubulin antibody to visualize the cytoplasm. More than 800 nuclei for each replicate were counted to calculate the fusion index (n was ≥3–5). Statistical analysis was performed using a one-way ANOVA Fisher-means comparison test in GraphPad Prism 9.

Prediction of pseudouridylation sites

We used the webserver tool snoGPS [31] to determine putative pseudouridylation sites that are mediated by SNORA40 and SNORA70 in mRNAs related to muscle differentiation. We selected as potential candidate sites those with a score >30. Indeed, snoGPS is a predictive tool, allowing you to test a candidate gene and predict its potential targeting snoRNAs, or to test a candidate snoRNA to predict its potential target RNAs. Candidate snoRNAs and genes of interest were tested individually. We selected a set of 10 prominent muscle-related genes and the top 10 upregulated nonmuscle-related genes from the total RNA-seq data and considered them as a set of random genes (Supplementary Fig. S3).

Nucleoli isolation

Nucleoli isolation was done as previously described [21]. A small amount of each fraction was saved and 2 μg of total RNA was reverse-transcribed from each. PCR assays were performed using equal amounts of cDNA from each fraction.

RNA pull-down

The primers are listed in Supplementary Table S1. MB was lysed with lysis buffer 50 mM Tris, pH 7.5, 0.3 M NaCl, 10 mM $MgCl_2$, 0.4% NP40), 120 U of RNase Inhibitor (New England Biolabs, USA), and 1× cOmplete Protease Inhibitor Cocktail tablets (Roche). Next, 140- and 98-bp fragments of the CCND3 cDNA containing the predicted sites guided by SNORA40 and SNORA70, respectively, were amplified by PCR. In addition, a T7 promoter was added at the 5′ end during the amplification. Both fragments were *in vitro* transcribed using the T7 RiboMax large-scale production system (Promega, Madison, WI, USA). Then, 400 pmol of SNORA40-RNA probe or SNORA70-RNA probe was annealed to 500 pmol of a biotinylated oligonucleotide complementary to SNORA40-RNA probe or SNORA70-RNA, respectively, in 50 mM KCl containing 1 U/μl RNaseOUT (Invitrogen), for 1 h at room temperature (RT). Based on the manufacturer's instructions, streptavidin Dynabeads™ M-280 (Thermo Fisher Scientific, USA) was washed twice with 0.1 M NaOH and 0.05 M NaCl and once in 0.1 M NaCl, and then precleared with 4 mg of cellular extract from MB in extract/clearing buffer (5% glycerol, 5 mM HEPES, pH 7, 5 mM Tris–HCl, pH 7.5, 75 mM KCl, 1 mM EDTA, 1M NaCl, 0.25% Triton X-100). The precleared beads were incubated with the RNA/oligonucleotide complex in binding/washing buffer (10 mM Tris–HCl, pH 7.5, 1 mM EDTA, 1 M NaCl) for 30 min at 4°C. Pre-incubated beads were washed twice in binding/washing buffer and added to 2 mg of cell extract from MB in RNA binding buffer (10% glycerol, 10 mM HEPES, pH 7, 150 mM KCl, 1 mM EDTA, 0.5% Triton X-100) containing 15 μg/ml yeast transfer RNA (tRNA), 1 mM DTT, and 240 U RNaseOut for 2 h at 4°C. The mixture was washed three times in RNA binding buffer, twice in lysis buffer, and once in RNA binding buffer. Finally, the beads were resuspended in Tri Reagent®. We performed a native RNA pull-down (i.e. conditions without Ultraviolet cross-linking), to maintain physiological conditions and to avoid proximal interactions that would not be direct.

Immunoprecipitation of pseudouridylated RNAs

IPs were performed as described previously, and the associated RNA was retrieved using the Tri Reagent® procedure [25]. Full-length CCND3 ivt + Ψ was *in vitro* transcribed using the HighYield T7 mRNA Synthesis Kit (Ψ-UTP, Jena Bioscience, Germany) before IP.

Results

Reduced levels of snoRNAs in DM1 cells compared with normal MB

Using RNA-seq on size-fractionated RNAs (>50 nt and <200 nt) from normal MB and their differentiated counterparts or MT, we identified all the annotated snoRNAs (www-snorna.biotoul.fr) and 100 new and not yet annotated snoRNA candidates, including new members of the known snoRNA families ([GEO GSE178649] and [21]). We focused our study on two known families of snoRNAs, SNORA40, and SNORA70, in which we identified new members that were expressed at lower levels in DM1 myoblasts (DM) compared with normal MB ([Fig. 1] and [GEO GSE269301]). The selection of these two families was arbitrary but influenced by two factors: (i) SNORA40 and SNORA70 are large families as annotated in Rfam [32] and in snoDB, the new reference database for snoRNAs [33]; and (ii) new members of these families are still being discovered within the human genome, like from our unbiased sequencing approach [21], which identified two new members for SNORA40, i.e. located at distinct genomic positions (Supplementary Table S3; alignment Supplementary Fig. S4). The slight differences in terms of sequence and structure are provided in Supplementary Fig. S5. For the SNORA70 family, two new members have been annotated in both databases since the beginning of our study, but we uncovered one additional member (Supplementary Table S1), also located at a different genomic position (Supplementary Fig. S6), with slight differences in structure and sequence (Supplementary Fig. S7).

From the medium RNA-seq (i.e. small RNAs from 50 to 200 nt) [21], we observed that the SNORA40 and SNORA70 families were highly expressed in normal MB and MT, with a slight increase in MT compared with MB. In contrast, they were expressed at low levels in DM cells (Fig. 1A and Supplementary Table S2). Reads mapping of these snoRNAs revealed boundaries typically found for other small RNAs, indicating that they are not irrelevant splicing byproducts but genuine RNA species.

From the total RNA-seq (GSE178649 and GSE227349) analysis, we confirmed that all genes hosting a SNORA40/70 member were expressed in both MB and DM cells, which is a prerequisite for splicing-dependent snoRNA production, as SNORA expression relies on host gene expression and splicing. These data suggest that the reduced levels of snoRNAs result from deregulated posttranscriptional events, as previously described [34]. Of note, the background of intron retention observed using IRFinder 2.0 [35] was slightly higher in DM cells compared with that in MB cells but cannot alone explain the reduction in snoRNA levels in DM1 MB. Where possible, we performed a few variant PCRs (using specific 3′-oligonucleotides) on small RNA fractionated on a column (<200 nt) and observed an overall decrease in DM cells compared with normal cells (Fig. 1B and C). Importantly, this was not because of a host gene expression defect as shown in Supplementary Fig. S8. TAF1D was fully expressed (Supplementary Fig. S8A) in MB as in DM1 cells. The levels of six out of the eight snoRNAs embedded within the introns of TAF1D were not affected (Supplementary Fig. S8B), whereas

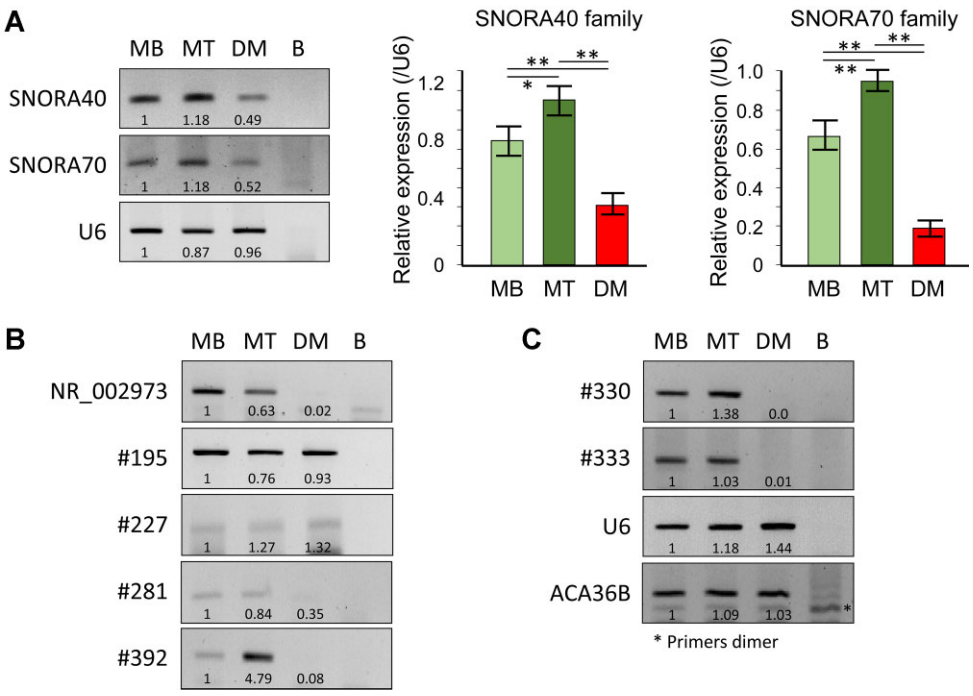

Figure 1. Newly identified snoRNAs are expressed less in DM1 cells. (**A**) PCR on a short RNA fraction using degenerated primers to amplify all members of the SNORA40 and SNORA70 families. Histograms represent the relative quantitation by Quantity One software corrected with U6 ($n = 3$). (**B**) PCR on a short RNA fraction using specific primers to amplify a single member of the SNORA40 family. (**C**) PCR on a short RNA fraction using specific primers to amplify a single member of the SNORA70 family. MB, normal myoblast; MT, normal myotubes; DM1, patient's MB; B, blank PCR. Error bars represent the standard error of the mean (SEM). *, $P < .05$; **, $P < .01$. Statistical analyses were performed using an unpaired *t*-test.

the levels of SNORD6 increased and that of SNORA40 decreased in MB versus DM1 cells. Hence, the six invariant snoRNAs provided ideal controls to suggest that global splicing defects in DM1 do not necessarily impact all snoRNA levels and that an unknown mechanism may affect the biogenesis of SNORA40 in DM1 cells.

SNORA40 and SNORA70 are required for myogenic differentiation

Since the family of SNORA40 is highly expressed in normal muscle cells (MB and MT) and greatly reduced in DM muscle cells, we first performed a loss-of-function analysis of the snoRNA families in normal MB to determine their relevance to myogenic differentiation. We used a combination of five ASO gapmers along with the consensus sequence of the snoRNA family of interest, thus not distinguishing members within the same family. We successfully reduced global levels of the entire SNORA40 family by 90% (Supplementary Fig. S2). After 24 h of knockdown, we switched the cell culture media to differentiate MB into MT. We then measured the expression of myogenic and cell-cycle markers and the ability to fuse into MT over 5 days (Fig. 2). Knockdown of the SNORA40 family resulted in a 60% decrease in the cell fusion index compared with control conditions (ASO gapmer targeting the luciferase mRNA; Fig. 2A and B). In addition, whereas the levels of CCND3 and MRF Myogenin (MYOG) mRNAs are known to increase during normal muscle differentiation [36, 37], depletion of the SNORA40 family resulted in reduced levels of these muscle and cell-cycle markers compared with the control conditions (Fig. 2C). In contrast, knockdown of the SNORA40 family had little or no impact on the levels of Cyclin B1 (CCNB1) and Myogenic factor 5 (MYF5) mRNAs (Fig. 2D), indicating that the transition between proliferating and differentiating states of the muscle cells [38] was not affected. Overall, SNORA40 family knockdown in normal muscle cells causes muscle differentiation defects, which are accompanied by reduced expression of muscle-specific markers and cell fusion events, whereas the commitment steps (before the formation of MT) occur normally.

The same effects on the fusion of normal MB were observed when using ASOs directed against the SNORA70 family (Fig. 2E and F). However, the four markers, except MYF5 mRNA levels at D0, did not vary between the control and ASO conditions (Fig. 2G and H). Thus, the decrease in cell fusion during the differentiation of normal MB depleted of SNORA70 was not caused by impaired expression of these markers as observed following SNORA40 knockdown. Therefore, SNORA70 may be involved in other or later processes, such as cell fusion. We assessed the mRNA levels of MyoMaker and Myomixer, which are known to promote myoblast fusion [39, 40]. Unfortunately, we did not observe any variation in kinetics over 5 days (Supplementary Fig. S9). This may also result from the 5-day kinetics, which may be too short to observe any variation (normal time is ~10 days).

Restoring SNORA40 or SNORA70 rescues cell fusion defects in DM muscle cells

Because the SNORA40 family was markedly reduced in DM1 MB, we attempted to rescue the snoRNA levels in these cells using a snoRNA-split-GFP expression vector. This was based on the insertion of a chimeric intron containing a snoRNA of interest or a random control sequence cloned into the split coding sequence of the eGFP. DM1 MB were electroporated with the plasmid of interest and induced to differentiate to

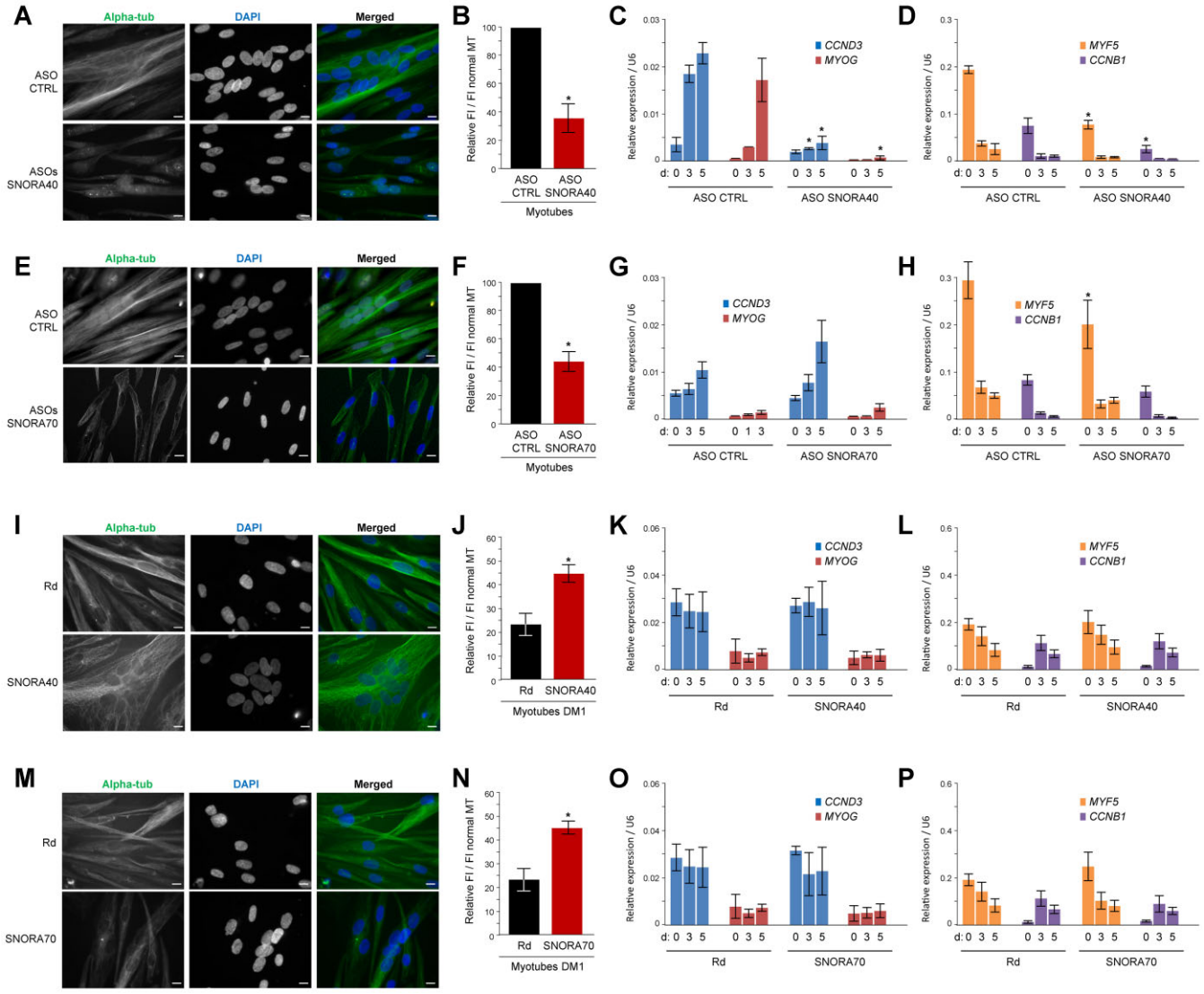

Figure 2. Functional studies of SNORA40 and SNORA70 in muscle cells. Immunofluorescence in normal MT with (ASO CTRL) or without (ASOs SNORA40 and SNORA70) the presence of (**A**) SNORA40 and (**E**) SNORA70 ($n \geq 3$). Relative fusion index measured at 5 days post-differentiation after the loss of (**B**) SNORA40 and (**F**) SNORA70 in normal muscle cells. More than 800 nuclei per replicate were counted to calculate the fusion index ($n \geq 3$). Relative expression of the CCND3 and MYOG mRNA differentiation markers in normal muscle cells depleted in (**C**) SNORA40 and (**G**) SNORA70 ($n \geq 3$). Relative expression of the MYF5 and CCNB1 mRNA proliferation markers in normal muscle cells depleted in (**D**) SNORA40 and (**H**) SNORA70 ($n \geq 3$). Immunofluorescence in DM1 MT with plasmids expressing either a random sequence (Rd), (**I**) SNORA40 (SNORA40), or (**M**) SNORA70 ($n \geq 3$). Relative to the fusion index measured at 5 days post-differentiation after the gain of (**J**) SNORA40 and (**N**) SNORA70 in DM1 muscle cells. More than 800 nuclei per replicate were counted to calculate the fusion index ($n \geq 3$). Relative expression of the CCND3 and MYOG mRNA differentiation markers in DM1 muscle cells expressing (**K**) SNORA40 and (**O**) SNORA70 ($n \geq 3$). Relative expression of the MYF5 and CCNB1 mRNA proliferation markers in DM1 muscle cells expressing (**L**) SNORA40 and (**P**) SNORA70 ($n \geq 3$). ASO, gapmers; CTRL, control; Alpha-tub, alpha-tubulin; FI, fusion index; U6, RNU6; CCND3, Cyclin D3; MYOG, Myogenin; MYF5, Myogenic factor 5; CCNB1, Cyclin B1; d, day of differentiation. Scale bar = 10 μm. Error bars represent the standard error of the mean (SEM). * indicates *P*-value < .05. Significant differences were assessed by comparing the two conditions: ASO CTRL versus ASO SNORA40 at each corresponding time point. Statistical analyses were performed using a one-way ANOVA Fisher-means comparison test for the FI results and a two-way ANOVA Tukey's multiple comparisons test for the qPCR results.

(i) estimate the percentage of electroporated cells by monitoring eGFP fluorescence by microscopy, and (ii) determine the effect of individual SNORA40 (NR_002973.1) or SNORA70 (NR_000011) members on the differentiation process in a more native approach, because it reproduces the postsplicing biogenesis of a snoRNA (lariat debranching and maturation steps). Under control conditions (i.e. DM1 MB electroporated with a plasmid expressing a random sequence within the context of a chimeric intron; see the "Material and methods" section), DM1 MT exhibited rare fusion events, which were reflected by a low relative fusion index (25%, Fig. 2I and J). However, DM1 cells expressing an ectopic SNORA40 member (NR_002973.1) formed multinucleated cells with a twofold increase in the fusion index (Fig. 2K and L). Of note, when ectopically expressing a single SNORA40 member, the majority of the DM1 multinucleated cells had only two nuclei and occasionally, three nuclei. Using the same procedure, restoring the levels of a single SNORA70 member (NR_000011) in DM1 cells increased the fusion index twofold compared with the control conditions, although cells with

three or more nuclei were more frequently observed compared with that of the SNORA40 member (NR_002973.1) (Fig. 2M and N). Moreover, ectopic SNORA40 and SNORA70 expression levels in DM cells were similar to those observed in control MB (Supplementary Fig. S10).

We assumed that the restoration of a single snoRNA would not be sufficient to fully rescue the cell fusion defects in DM1. Therefore, we attempted to restore the RNA levels of both SNORA40 and SNORA70 in DM1 cells and rescue the cell fusion defects in DM1. The fusion index increased by a factor of three, when both SNORA40 and SNORA70 members were coexpressed (Fig. 3A and C), suggesting a synergistic effect of these two snoRNAs from two different families. As mentioned previously, the population of DM1 MT expressing SNORA40 and SNORA70 is similar to the one expressing SNORA40 alone, with the only difference being that more cells with two nuclei were observed (Fig. 2). This difference could be explained by a higher fusion index in cells electroporated with the two snoRNAs compared with those with SNORA40 alone, and an additive effect is speculated. When used in combination, SNORA40 and SNORA70 plasmids were co-transfected with half of the material (2.5 μg of each plasmid) to maintain a total amount of 5 μg of transfected plasmids (5 μg). Therefore, the synergistic effect results from the action of the two snoRNAs and not from a greater quantity of snoRNAs. Of interest, as shown in Fig. 3B, when DM cells were electroporated with SNORA70, there were more cells with three nuclei and greater than SNORA40 alone ($P < .05$, red lines). This suggests that SNORA40 and SNORA70 were not playing the same role on the same pathway.

Modification of pseudouridylation levels in DM1 compared with those in normal cells

We quantified global pseudouridylation levels from normal and pathological primary cells using liquid chromatography-tandem mass spectrometry (LC-MS/MS). Although not statistically significant, we found a trend toward decreased global pseudouridylation levels in DM1 patients' versus normal cells [8.7 ± 0.4 versus 11.6 ± 2.7, respectively (Supplementary Fig. S11; pseudouridine levels expressed in percentage of modification per adenine)]. This result was far from the anecdotal given the number of RNAs being targeted by snoRNAs for modification.

CCND3 mRNA was identified as a target of SNORA40 and SNORA70

Using snoGPS [31] as an *in silico* tool to predict pseudouridylation (Ψ) sites targeted by SNORA40 or SNORA70, we uncovered two potential sites on CCND3 mRNA, which is involved in muscle differentiation (CCND3, RefSeq NM_001760) (Fig. 4A and B). Since these two sites on CCND3 mRNA were predictions, we tested additional transcripts relevant or not to muscle differentiation using snoGPS (Supplementary Fig. S3). Almost all the tested transcripts scored 0 when we searched for binding sites for SNORA40 and SNORA70, except for the TGFBI transcript, for which the prediction score for SNORA70 was 26.92 (Supplementary Fig. S3). When a threshold of 30 for the snoGPS score (used in the work of Schattner *et al.* [32] for discovering new snoRNAs) was applied, the TGFBI transcript was not considered for subsequent analyses. Therefore, the two predicted sites for SNORA40 (score 30.82) and SNORA70 (score 44.34) made the CCND3 transcript a good candidate for the rest of the study. SNORA40 targets a site located at the 3′-UTR of CCND3 mRNA, whereas the site for SNORA70 is located in the CDS. Most human SNORAs are composed of two stem-loops at the 5′ and 3′ ends, with an adjacent ACA box. Hence, SNORAs are theoretically capable of guiding pseudouridylation at two different sites simultaneously [41]. Importantly, in contrast to other rRNAs, the predicted Ψ sites on CCND3 mRNA were mediated by the 5′ stem of SNORA40 and SNORA70 instead of the 3′ stem (Supplementary Fig. S12).

As the process by H/ACA snoRNAs occurs in the nucleoli, we determined whether CCND3 mRNA was present in this compartment [42]. Using cell fractionation, as previously described [21], we showed that a small proportion of CCND3 mRNA was located in the nucleolar fraction (Fig. 4C).

To determine whether a direct interaction occurs between SNORAs and CCND3, we used an RNA pull-down assay with biotinylated complementary oligonucleotides [25] to precipitate CCND3 mRNA and its associated sncRNAs (see the "Material and methods" section). Using a candidate approach, specific primers were designed to detect SNORA40 and SNORA70 in the precipitate. As shown in Fig. 4D and E, neither RNU6 (U6) nor SNORA36B (ACA36B) was co-precipitated with CCND3 mRNA. In contrast, the SNORA40 (Fig. 4D) and SNORA70 families (Fig. 4E) were associated with CCND3 mRNA.

Next, we determined whether CCND3 mRNA was pseudouridylated by immunoprecipitation with a pseudouridine-specific antibody [43]. As our starting material, we used a sample enriched in polyA+ mRNA with significantly reduced rRNA. As shown in Fig. 4F, even the residual 18S rRNA was successfully immunoprecipitated, which served as a positive control. The SH3 domain binding glutamate rich protein like 3 (SH3BGRL3) mRNA was used as a negative control because no SNORA40 and SNORA70 sites were predicted by snoGPS in its mRNA sequence. As expected, CCND3 mRNA, but not SH3BGRL3, was efficiently immunoprecipitated using a Ψ antibody, but not using an irrelevant non-specific anti-Xpress antibody (IgG control). As an additional control, we used *in vitro*-synthesized CCND3 transcripts using a T7 normal kit or a T7 Ψ kit (which incorporates Ψ nucleotides into the *in vitro* transcript) and performed isolated probe (IP)-PCR *in vitro* using 1 μg of *in vitro* transcript and 1 μg of antibody (input 5%). As expected, only the Ψ CCND3 transcript was pulled down by the anti-antibody (Fig. 4F). We also tried the CMCT method (*N*-cyclohexyl-*N*'-(2-morpholinoethyl)carbodiimide treatment) [44] to precisely identify nucleotides that were pseudouridylated, but without any success. However, the results were inconclusive, which was likely the result of the low relative abundance of CCND3 mRNA within the total mRNA population (data not shown).

Furthermore, qPCR was performed, which showed no difference in CCND3 mRNA levels between the control conditions and the conditions in which SNORA40 and/or SNORA70 were electroporated (Supplementary Fig. S13). We also performed a western blot analysis (Fig. 5A) to compare the expression of CCND3 protein between MB and DM myoblasts and confirm that DM cells did not express CCND3 as previously shown [45]. When DM1 was electroporated with plasmids containing the split-GFP and SNORA40 and SNORA70, we restored CCND3 protein expression levels

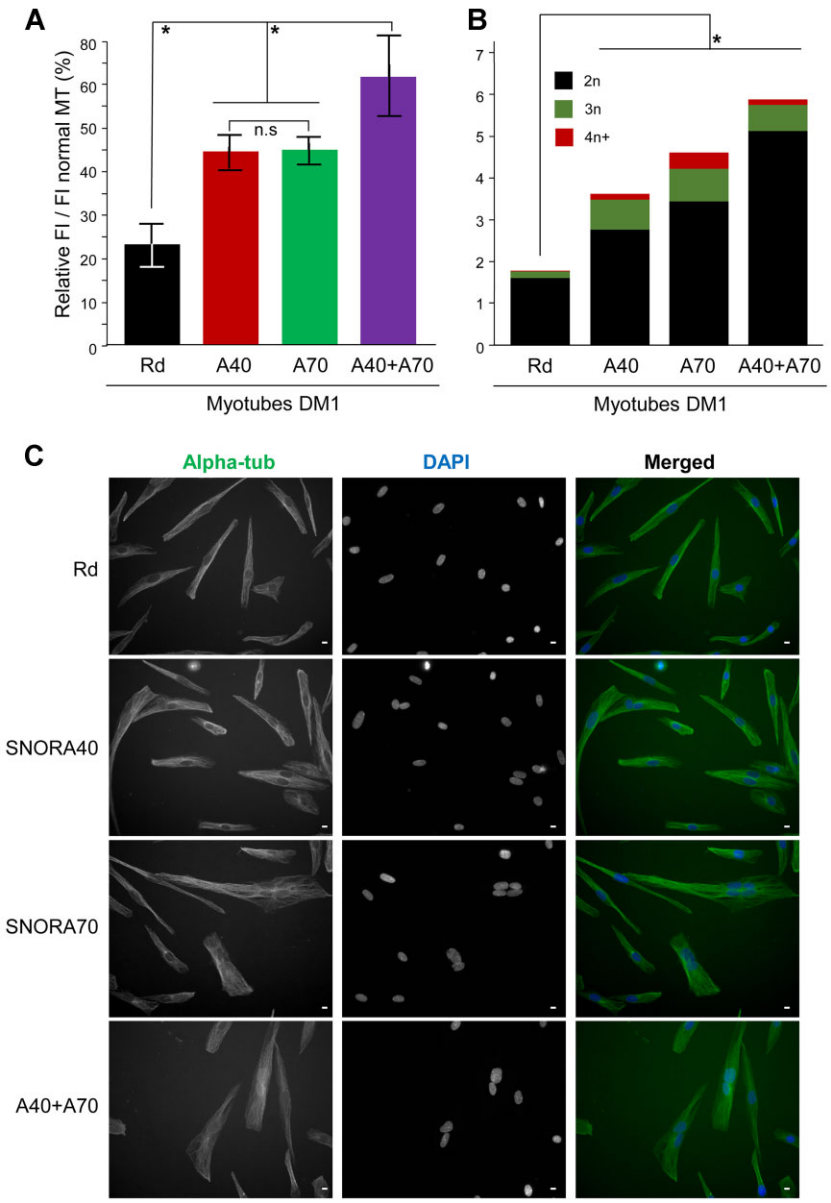

Figure 3. Synergic effect of a gain-of-function for both SNORA40 and SNORA70 during muscle differentiation. (**A**) Relative to the fusion index measured at 5 days post-differentiation (data corresponding to the condition Rd, A40, and A70 are identical to those in Fig. 2). More than 800 nuclei per replicate were counted to calculate the fusion index ($n \geq 3$). (**B**) Percentage of cells displaying multinucleated cells with two nuclei (2n), three nuclei (3n), or more than three nuclei (4n+) ($n \geq 3$). (**C**) Immunofluorescence in normal MT with plasmids expressing either a random sequence (Rd), SNORA40 (SNORA40, A40), SNORA70 (SNORA70, A70), or both SNORA40 and SNORA70 (A40 + A70) ($n \geq 3$). Alpha-tub, alpha-tubulin; FI, fusion index; U6, RNU6; CCND3. Scale bar = 10 μm. Error bars represent the standard error of the mean (SEM). * indicates *P*-value < .05. Statistical analyses were performed using a one-way ANOVA Fisher-means comparison test and an unpaired *t*-test for panel (B).

(Fig. 5A and Supplementary Fig. S13), suggesting a role of SNORA40 and/or SNORA70 in the stability/translation of CCND3 mRNA.

We then decided to block pseudouridylation using ASOs that obstruct the Ψ sites of CCND3. Briefly, we used the ASOs listed in Supplementary Table S1 in normal MB, to compete with SNORA40 or SNORA70 binding without affecting CCND3 mRNA stability. Whereas ASOs can promote RNA degradation, as is the case for the one against the SNORA70 Ψ site, we found that the one directed against the SNORA40 Ψ site did not affect CCND3 mRNA levels (Supplementary Fig. S13B). Interestingly, western blot analysis of proteins extracted from normal MB treated with this ASO showed marked effects on CCND3 protein levels compared to cells treated with the control ASO (Fig. 5C).

Taken together, our data strongly suggest a model in which restoring SNORA40/70 levels in DM1 MB restores their differentiation capacity, to some extent, through the pseudouridylation of CCND3 mRNA and increased levels of the protein, which is required for cell-cycle exit before commitment to differentiation.

Discussion

In this study, we identified snoRNA members of the SNORA40 and SNORA70 families that were specifically

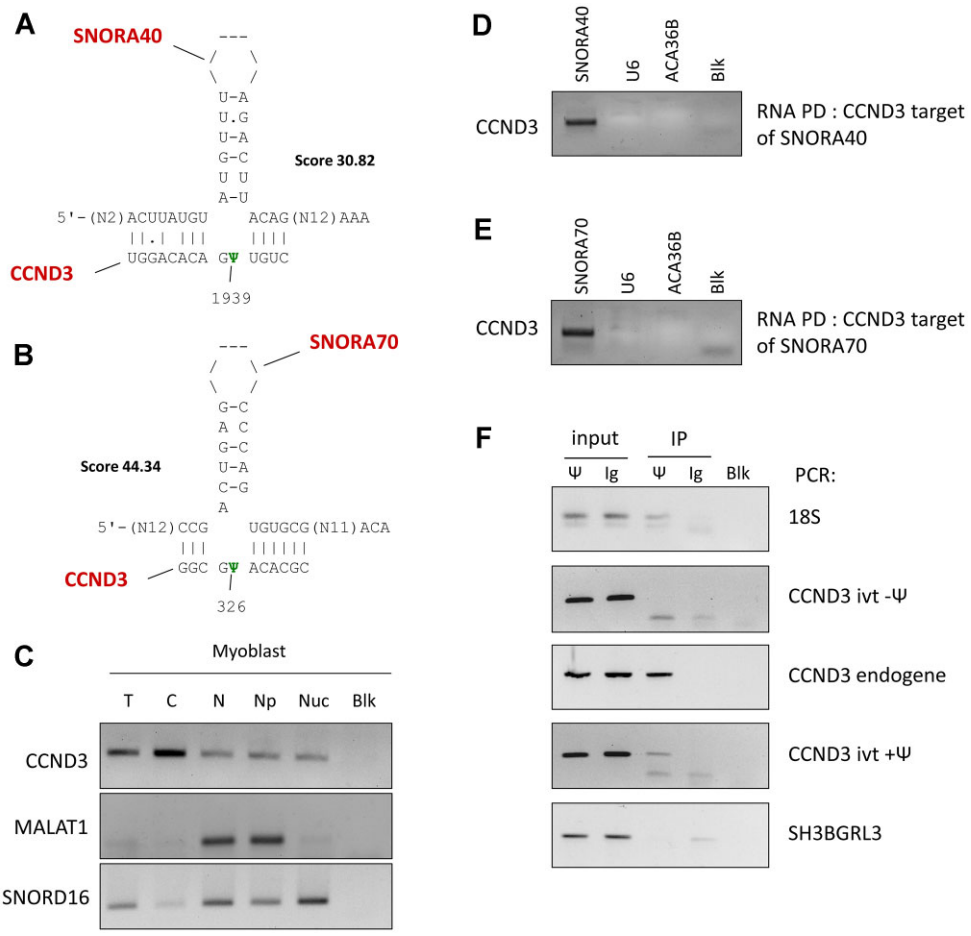

Figure 4. Interaction of CCND3 with SNORA70 and SNORA40. (**A** and **B**) Physical interaction of CCND3 with SNORA40 and SNORA70, respectively, as predicted with snoGPS software. Scores are indicated in bold. (**C**) The accumulation of CCND3 in the nucleoli. Isolation of nucleoli by sucrose cushion centrifugation was performed as described in [36]. The total RNA from each fraction was extracted and the localization of *CCND3* mRNA was assessed by RT-PCR ($n = 2$). To confirm the correct isolation of the nucleoli, MALAT1 RNA and SNORD16 were used as nuclear (negative control) and nucleolar (positive control) markers, respectively. cDNA (50 ng of equivalent RNA) was used for each PCR reaction. (**D** and **E**) Direct interaction of CCND3 with SNORA40 and SNORA70, respectively. U6 and ACA36B were used as negative controls ($n = 2$). (**F**) Immunoprecipitation (1 μg of RNA) of Psi in mRNA-enriched populations followed by RT-PCR. Five percent of the input was used. *In vitro* transcribed CCND3 RNA with and without pseudouridines were used as positive and negative controls, respectively ($n = 3$). Ψ, Psi; T, total fraction; C, cytoplasmic fraction; N, nuclear fraction; Np, nucleoplasmic fraction; Nuc, nucleolar fraction; Blk, mock PCR; RNA PD, RNA pull-down; IP, Immunoprecipitation; Ig, immunoglobulin; 18S, rRNA 18S; SH3BGRL3, SH3 domain binding glutamic acid-rich-like protein 3.

downregulated in muscle progenitor cells from patients with DM1 (Supplementary Table S2). Importantly, restoring their normal levels by gain-of-function experiments was sufficient to counteract, at least partially, the impaired differentiation that characterizes cells from DM1 patients. From a mechanistic point of view, we showed that SNORA40/70 operate at a posttranscriptional level, through the pseudouridylation of CCND3 mRNA, with a striking impact on the production of the CCND3 protein, which is required for the commitment of MB toward muscle differentiation. Thus, our work provides new lines of research whereby snoRNAs can be leveraged to correct, at least partially, the disease phenotypes in splicing diseases.

Our previous medium RNA-seq data [21] revealed that SNORA40 and SNORA70 family levels increased during normal muscle differentiation but were markedly reduced in cells from patients with DM1. Although DM1 is caused by splicing defects, snoRNA level variations did not correlate with changes in host gene expression or AS, suggesting a defective posttranscriptional regulatory mechanism in snoRNA biogenesis [34]. Overall, our results align with those previously published in the literature showing that snoRNA levels are dynamic and undergo a certain degree of regulation depending on the state of the cell, notably during cell differentiation [17, 46]. For example, certain snoRNAs are crucial for normal B-cell differentiation in humans [47]. In mice, a dozen H/ACA snoRNAs have been observed to be regulated during muscle differentiation [46]. Thus, snoRNA deregulation in DM1 could represent a new biomarker class, similar to miRNAs [48], and may extend to other human diseases involving splicing defects [49–52].

To the best of our knowledge, this study is the first to show that the SNORA40 and SNORA70 families are essential for muscle differentiation. Notably, they appear to act synergistically, as ectopic expression of both families more effectively restores cell fusion defects in DM1 cells. Few studies have demonstrated the direct effect of snoRNAs on cell differentiation. For instance, SNORD126 promotes adipocyte differentiation by activating the PI3K-AKT pathway in rats [53]. Further research is needed to clarify the precise impact of

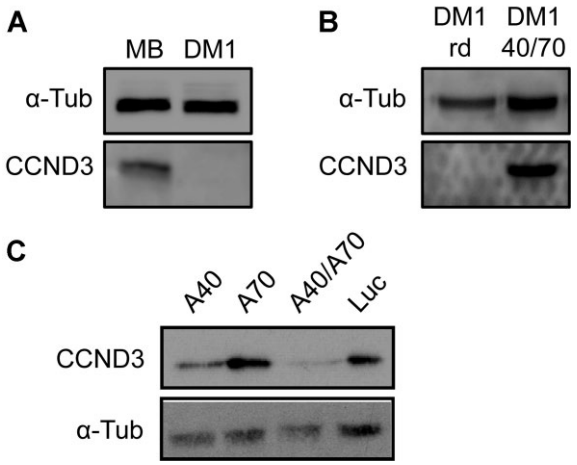

Figure 5. CCND3 expression in MB. (**A**) Expression of CCND3 in normal versus pathological MB ($n = 2$). Thirty μg of protein extract was used. (**B**) Expression of CCND3 in DM1 electroporated with a random sequence or with SNORA40/SNORA70 ($n = 2$). One hundred μg of protein extract was used. (**C**) Expression of CCND3 with or without blocking ASOs; 100 μg of protein extract was used ($n = 2$). α-tub, alpha-tubulin; CCND3, MB, normal myoblast; DM1, myoblast from DM1 patient; DM1 rd, DM1 electroporated with the random plasmid; DM1 40/70, DM1 electroporated with the SNORA40 and SNORA70 plasmids.

SNORA40 and SNORA70 on muscle differentiation and the transcriptome of differentiating cells, as these snoRNAs influence muscle differentiation–related gene expression and myotube formation differently. However, the commitment steps preceding pathological myotube formation likely remain intact, given that mRNA levels of proliferating myoblast markers (MYF5 and CCNB1) remained unchanged during differentiation (Fig. 2). Overall, our findings highlight snoRNAs' potential to counteract differentiation defects in DM1. SnoRNAs have already shown promise in correcting abnormal phenotypes in splicing diseases. For example, the human snoRNA Jouvence, which promotes cell proliferation and epithelial–mesenchymal transition, is a promising cancer therapy target [54]. Thus, snoRNAs represent a new class of therapeutic targets, particularly in diseases where RNA splicing (essential for snoRNA production) is impaired [54–57].

SnoRNAs primarily function as guides for RNA posttranscriptional modifications, particularly on rRNA, although a few mRNA targets have been identified [58]. Given that SNORAs, a snoRNA subgroup, guide pseudouridylation, we used snoGPS [31] to predict Ψ sites on mRNAs encoding known muscle differentiation markers. Our analysis identified CCND3 mRNA as a potential target, with one predicted Ψ site for each SNORA40 and SNORA70. This finding was notable, as CCND3 promotes cell-cycle exit, a crucial step in muscle differentiation. However, CCND3 may not be the primary target of these snoRNAs. Several observations support this notion: (i) the percentage reduction in snoRNAs when treated with ASO gapmers was not directly correlated with the equivalent phenotype observed; (ii) loss-of-function and gain-of-function experiments produced different marker responses under normal and pathological conditions; (iii) the fusion phenotype associated with SNORA70 gain-of-function resulted in an increased nuclei count, which would not be expected if the same targets were affected, so CCND3 was unlikely the main target for both snoRNAs; and (iv) the observed synergistic effects are difficult to reconcile with an identical target for the two snoRNAs unless both Ψ sites are required for function. Overall, these findings suggest that SNORA40 and SNORA70 contribute to the phenotype through distinct pathways. Additionally, differences in ASO-mediated blocking mechanisms, i.e. one preventing pseudouridylation and the other destabilizing RNA, further complicate interpretation. Although the phenotypic outcomes appear similar, they may not arise from the same molecular pathway.

It remains unclear whether the Ψ modification on CCND3 mRNA is stoichiometric or substoichiometric. However, we observed that only a subset of CCND3 mRNAs localized to the nucleolus, where snoRNA-mediated modifications occur (Fig. 4C). This localization may represent a transient stage in which the mRNAs are modified before transport to the cytoplasm for translation or other processes. However, from the present study, we established the following: (i) CCND3 mRNA levels are comparable between normal and pathological cells; (ii) when SNORA40 and/or SNORA70 are expressed (ectopically or physiologically), CCND3 protein is detectable; and (iii) under the same conditions, CCND3 mRNAs (or a subset) are pseudouridylated. Together, these findings suggest that at least a subset of CCND3 mRNAs undergoes pseudouridylation when CCND3 protein is present.

We attempted to use the CMCT method [44] to precisely identify pseudouridylated nucleotides and quantify pseudouridylated mRNA proportions. However, these efforts were unsuccessful, likely due to the low relative abundance of CCND3 mRNA within the total mRNA population. To date, only one study has successfully applied CMCT to human mRNAs [44].

Notably, Ψ modifications have been identified in mRNAs [15], but their functional significance remains debated (for a review, refer to [16, 59]). It is unclear whether pseudouridylation stabilizes mRNAs [60] or promotes their degradation [61]. As pseudouridines are distributed throughout mRNAs [15, 62], several studies have examined their role in translation. Pseudouridines can enhance protein output, although the underlying mechanism remains unknown [60, 63]. However, pseudouridylation within a codon may alter translation speed or mRNA decoding, ultimately affecting protein yield [64, 65]. Thus, the effects of pseudouridylation on mRNA likely depend on its location within the sequence and the specific codon affected. In the present study, SNORA70 guided pseudouridylation on a methionine codon at position 36 of CCND3 mRNA, whereas SNORA40 targeted the 3 UTR. Further research is needed to determine how these modifications influence CCND3 mRNA stability and translation. Overall, the reduced snoRNA levels and splicing defects observed in DM1 cells may lead to abnormal mRNA modifications, potentially disrupting translatability and ultimately altering cell fate.

In conclusion, our study provides new insights into the potential of snoRNA during myogenic differentiation and its alteration in DM1 disease. Furthermore, we demonstrated that at least two families of snoRNAs participate in the myogenic differentiation process, and their deregulation contributes to the cell fusion defects observed in DM1 muscle cells. Based on our findings and existing literature, these data pave the way for snoRNAs to be considered as new therapeutic targets for various pathologies, including cancer [57]. On a more specific and mechanistic side, our data identified SNORA40/70 families as regulators of CCND3 expression, a key factor of

muscle differentiation. This work provides, to our knowledge, the first indication of a link between snoRNAs and muscle physiology through posttranscriptional mRNA modification. Although preliminary, our results represent a step forward in exploring the role of snoRNAs in muscle cells and their involvement in gene expression regulation.

Acknowledgements

We would like to thank Dr Franck Letourneur and Juliette Hamroune (Platform GENOM'IC, Institut Cochin, France) for the RNA sequencing. We thank Dr Magali Hennion for the bioinformatics support provided at the Bioinformatics and Biostatistics Core Facility, Paris Epigenetics and Cell Fate Center. We also thank Drs Louis Chauvière and Damien Ulveling for their bioinformatic advice. We are also grateful to the Epigenomics Core Facility (Laure Ferry and Laurence Del Maestro), the Common Facilities (Myriam Mohamed and Sylvie Gatibelza), and the Administrative Management (Ingrid Citerne). Thanks to Phillipe Debiais for computer troubleshooting. We also thank the Myobank-AFM from Myology Institute (BB-0033-00012) and particularly, Drs Stéphane Vasseur and Maud Chapart.

Author contributions: B.B. and F.H. performed experiments, data analysis, and writing of the paper. H.B. and E.B. performed experiments and data analysis. F.H. and G.T. performed bioinformatic experiments. D.F. and V.M. constructed and provided the cells. C.F. performed data analysis and writing of the paper. All authors read the manuscript and made corrections.

Supplementary data

Supplementary data is available at NAR online.

Conflict of interest

None declared.

Funding

This work was supported by AFM (Association Française contre les Myopathies, #22341 and #24224). B.B. was supported by the AFM (#21363) and the LabEx "Who am I?" (#ANR-11-LABX-0071 and IDEX #ANR-18-IDEX-0001). Funding to pay the Open Access publication charges for this article was provided by French Muscular Dystrophy Association.

Data availability

Genomic data generated for this study have been deposited in the GEO repository with the accession numbers GSE227349 and GSE269301 or were taken from our previous work [21], under accession number GSE178649.

References

1. Brook JD, McCurrach ME, Harley HG *et al.* Molecular basis of myotonic dystrophy: expansion of a trinucleotide (CTG) repeat at the 3' end of a transcript encoding a protein kinase family member. *Cell* 1992;**68**:799–808. https://doi.org/10.1016/0092-8674(92)90154-5
2. Dansithong W, Paul S, Comai L *et al.* MBNL1 is the primary determinant of focus formation and aberrant insulin receptor splicing in DM1. *J Biol Chem* 2005;**280**:5773–80. https://doi.org/10.1074/jbc.M410781200
3. Miller JW, Urbinati CR, Teng-Umnuay P *et al.* Recruitment of human muscleblind proteins to (CUG)(n) expansions associated with myotonic dystrophy. *EMBO J* 2000;**19**:4439–48. https://doi.org/10.1093/emboj/19.17.4439
4. Lopez-Martinez A, Soblechero-Martin P, de-la-Puente-Ovejero L *et al.* An overview of alternative splicing defects implicated in myotonic dystrophy type I. *Genes* 2020;**11**: 1109. https://doi.org/10.3390/genes11091109
5. Isesele PO, Mazurak VC. Regulation of skeletal muscle satellite cell differentiation by omega-3 polyunsaturated fatty acids: a critical review. *Front Physiol* 2021;**12**:682091. https://doi.org/10.3389/fphys.2021.682091
6. Timchenko NA, Patel R, Iakova P *et al.* Overexpression of CUG triplet repeat-binding protein, CUGBP1, in mice inhibits myogenesis. *J Biol Chem* 2004;**279**:13129–39. https://doi.org/10.1074/jbc.M312923200
7. De LG, Ferretti R, Bruschi M *et al.* Cyclin D3 critically regulates the balance between self-renewal and differentiation in skeletal muscle stem cells. *Stem Cells* 2013;**31**:2478–91. https://doi.org/10.1002/stem.1487
8. De SF, Albini S, Mezzaroma E *et al.* pRb-dependent cyclin D3 protein stabilization is required for myogenic differentiation. *Mol Cell Biol* 2007;**27**:7248–65. https://doi.org/10.1128/MCB.02199-06
9. Chu CY, Lim RW. Involvement of p27(kip1) and cyclin D3 in the regulation of cdk2 activity during skeletal muscle differentiation. *Biochim Biophys Acta Mol Cell Res* 2000;**1497**:175–85. https://doi.org/10.1016/S0167-4889(00)00064-1
10. Ishido M. Cyclin D3 colocalizes with myogenin and p21 in skeletal muscle satellite cells during early-stage functional overload. *Acta Histochem Cytochem* 2023;**56**:111–9. https://doi.org/10.1267/ahc.23-00041
11. Baldini L, Charpentier B, Labialle S. Emerging data on the diversity of molecular mechanisms involving C/D snoRNAs. *Noncoding RNA* 2021;**7**:30.
12. Decatur WA, Fournier MJ. rRNA modifications and ribosome function. *Trends Biochem Sci* 2002;**27**:344–51. https://doi.org/10.1016/S0968-0004(02)02109-6
13. Tollervey D, Lehtonen H, Jansen R *et al.* Temperature-sensitive mutations demonstrate roles for yeast fibrillarin in pre-rRNA processing, pre-rRNA methylation, and ribosome assembly. *Cell* 1993;**72**:443–57. https://doi.org/10.1016/0092-8674(93)90120-F
14. Zebarjadian Y, King T, Fournier MJ *et al.* Point mutations in yeast CBF5 can abolish *in vivo* pseudouridylation of rRNA. *Mol Cell Biol* 1999;**19**:7461–72. https://doi.org/10.1128/MCB.19.11.7461
15. Carlile TM, Rojas-Duran MF, Zinshteyn B *et al.* Pseudouridine profiling reveals regulated mRNA pseudouridylation in yeast and human cells. *Nature* 2014;**515**:143–6. https://doi.org/10.1038/nature13802
16. Borchardt EK, Martinez NM, Gilbert WV. Regulation and function of RNA pseudouridylation in human cells. *Annu Rev Genet* 2020;**54**:309–36. https://doi.org/10.1146/annurev-genet-112618-043830
17. Warner WA, Spencer DH, Trissal M *et al.* Expression profiling of snoRNAs in normal hematopoiesis and AML. *Blood Adv* 2018;**2**:151–63. https://doi.org/10.1182/bloodadvances.2017006668
18. Yang X, Li Y, Li L *et al.* SnoRNAs are involved in the progression of ulcerative colitis and colorectal cancer. *Dig Liver Dis* 2017;**49**:545–51. https://doi.org/10.1016/j.dld.2016.12.029
19. Hoelscher SC, Doppler SA, Dressen M *et al.* MicroRNAs: pleiotropic players in congenital heart disease and regeneration. *J Thorac Dis* 2017;**9**:S64–81. https://doi.org/10.21037/jtd.2017.03.149

20. Mei YP, Liao JP, Shen J *et al.* Small nucleolar RNA 42 acts as an oncogene in lung tumorigenesis. *Oncogene* 2012;**31**:2794–804. https://doi.org/10.1038/onc.2011.449
21. Bogard B, Francastel C, Hube F. Systematic identification and functional validation of new snoRNAs in human muscle progenitors. *Noncoding RNA* 2021;**7**:56. https://doi.org/10.3390/ncrna7030056
22. Zhang X, Jonassen I. RASflow: an RNA-seq analysis workflow with Snakemake. *BMC Bioinformatics* 2020;**21**:110. https://doi.org/10.1186/s12859-020-3433-x
23. Kim D, Paggi JM, Park C *et al.* Graph-based genome alignment and genotyping with HISAT2 and HISAT-genotype. *Nat Biotechnol* 2019;**37**:907–15. https://doi.org/10.1038/s41587-019-0201-4
24. Liao Y, Smyth GK, Shi W. The R package Rsubread is easier, faster, cheaper and better for alignment and quantification of RNA sequencing reads. *Nucleic Acids Res* 2019;**47**:e47. https://doi.org/10.1093/nar/gkz114
25. Hube F, Ulveling D, Sureau A *et al.* Short intron-derived ncRNAs. *Nucleic Acids Res* 2017;**45**:4768–81. https://doi.org/10.1093/nar/gkw1341
26. Abelson J, Trotta CR, Li H. tRNA splicing. *J Biol Chem* 1998;**273**:12685–8. https://doi.org/10.1074/jbc.273.21.12685
27. Ferri F, Bouzinba-Segard H, Velasco G *et al.* Non-coding murine centromeric transcripts associate with and potentiate Aurora B kinase. *Nucleic Acids Res* 2009;**37**:5071–80. https://doi.org/10.1093/nar/gkp529
28. Liang XH, Shen W, Crooke ST. Efficient and selective knockdown of small non-coding RNAs. *Methods Mol Biol* 2015;**1296**:203–11. https://doi.org/10.1007/978-1-4939-2547-6_19
29. Kittler R, Surendranath V, Heninger AK *et al.* Genome-wide resources of endoribonuclease-prepared short interfering RNAs for specific loss-of-function studies. *Nat Methods* 2007;**4**:337–44. https://doi.org/10.1038/nmeth1025
30. Hedouin S, Grillo G, Ivkovic I *et al.* CENP-A chromatin disassembly in stressed and senescent murine cells. *Sci Rep* 2017;**7**:42520. https://doi.org/10.1038/srep42520
31. Schattner P, Brooks AN, Lowe TM. The tRNAscan-SE, snoscan and snoGPS web servers for the detection of tRNAs and snoRNAs. *Nucleic Acids Res* 2005;**33**:W686–9. https://doi.org/10.1093/nar/gki366
32. Kalvari I, Nawrocki EP, Ontiveros-Palacios N *et al.* Rfam 14: expanded coverage of metagenomic, viral and microRNA families. *Nucleic Acids Res* 2021;**49**:D192–200. https://doi.org/10.1093/nar/gkaa1047
33. Bergeron D, Paraqindes H, Fafard-Couture E *et al.* snoDB 2.0: an enhanced interactive database, specializing in human snoRNAs. *Nucleic Acids Res* 2023;**51**:D291–6. https://doi.org/10.1093/nar/gkac835
34. Fafard-Couture E, Bergeron D, Couture S *et al.* Annotation of snoRNA abundance across human tissues reveals complex snoRNA-host gene relationships. *Genome Biol* 2021;**22**:172. https://doi.org/10.1186/s13059-021-02391-2
35. Lorenzi C, Barriere S, Arnold K *et al.* IRFinder-S: a comprehensive suite to discover and explore intron retention. *Genome Biol* 2021;**22**:307. https://doi.org/10.1186/s13059-021-02515-8
36. Cusella-De Angelis MG, Lyons G, Sonnino C *et al.* MyoD, myogenin independent differentiation of primordial myoblasts in mouse somites. *J Cell Biol* 1992;**116**:1243–55. https://doi.org/10.1083/jcb.116.5.1243
37. Kiess M, Gill RM, Hamel PA. Expression of the positive regulator of cell cycle progression, cyclin D3, is induced during differentiation of myoblasts into quiescent myotubes. *Oncogene* 1995;**10**:159–66.
38. Rudnicki MA, Jaenisch R. The MyoD family of transcription factors and skeletal myogenesis. *Bioessays* 1995;**17**:203–9. https://doi.org/10.1002/bies.950170306
39. Bi P, Ramirez-Martinez A, Li H *et al.* Control of muscle formation by the fusogenic micropeptide myomixer. *Science* 2017;**356**:323–7. https://doi.org/10.1126/science.aam9361
40. Millay DP, O'Rourke JR, Sutherland LB *et al.* Myomaker is a membrane activator of myoblast fusion and muscle formation. *Nature* 2013;**499**:301–5. https://doi.org/10.1038/nature12343
41. Reichow SL, Hamma T, Ferre-D'Amare AR *et al.* The structure and function of small nucleolar ribonucleoproteins. *Nucleic Acids Res* 2007;**35**:1452–64. https://doi.org/10.1093/nar/gkl1172
42. Narayanan A, Lukowiak A, Jady BE *et al.* Nucleolar localization signals of box H/ACA small nucleolar RNAs. *EMBO J* 1999;**18**:5120–30. https://doi.org/10.1093/emboj/18.18.5120
43. Mishima E, Jinno D, Akiyama Y *et al.* .. Immuno-northern blotting: detection of RNA modifications by using antibodies against modified nucleosides. *PLoS One* 2015;**10**:e0143756. https://doi.org/10.1371/journal.pone.0143756
44. Zhang W, Eckwahl MJ, Zhou KI *et al.* Sensitive and quantitative probing of pseudouridine modification in mRNA and long noncoding RNA. *RNA* 2019;**25**:1218–25. https://doi.org/10.1261/rna.072124.119
45. Salisbury E, Sakai K, Schoser B *et al.* Ectopic expression of cyclin D3 corrects differentiation of DM1 myoblasts through activation of RNA CUG-binding protein. *Exp Cell Res* 2008;**314**:2266–78. https://doi.org/10.1016/j.yexcr.2008.04.018
46. McCann KL, Kavari SL, Burkholder AB *et al.* H/ACA snoRNA levels are regulated during stem cell differentiation. *Nucleic Acids Res.* 2020;**48**:8686–703. https://doi.org/10.1093/nar/gkaa612
47. Verbeek MWC, Erkeland SJ, van der Velden V. Dysregulation of small nucleolar RNAs in B-cell malignancies. *Biomedicines* 2022;**10**:1229. https://doi.org/10.3390/biomedicines10061229
48. Perfetti A, Greco S, Cardani R *et al.* Validation of plasma microRNAs as biomarkers for myotonic dystrophy type 1. *Sci Rep* 2016;**6**:38174. https://doi.org/10.1038/srep38174
49. Chen X, Ba Y, Ma L *et al.* Characterization of microRNAs in serum: a novel class of biomarkers for diagnosis of cancer and other diseases. *Cell Res* 2008;**18**:997–1006. https://doi.org/10.1038/cr.2008.282
50. Zhu W, Zhang T, Luan S *et al.* Identification of a novel nine-SnoRNA signature with potential prognostic and therapeutic value in ovarian cancer. *Cancer Med* 2022;**11**:2159–70. https://doi.org/10.1002/cam4.4598
51. Zhao Y, Yan Y, Ma R *et al.* Expression signature of six-snoRNA serves as novel non-invasive biomarker for diagnosis and prognosis prediction of renal clear cell carcinoma. *J Cell Mol Med* 2020;**24**:2215–28. https://doi.org/10.1111/jcmm.14886
52. Ding Y, Sun Z, Zhang S *et al.* Identification of snoRNA SNORA71A as a novel biomarker in prognosis of hepatocellular carcinoma. *Dis Markers* 2020;**2020**:8879944. https://doi.org/10.1155/2020/8879944
53. He Y, Wu Y, Mei B *et al.* A small nucleolar RNA, SNORD126, promotes adipogenesis in cells and rats by activating the PI3K-AKT pathway. *J Cell Physiol* 2021;**236**:3001–14. https://doi.org/10.1002/jcp.30066
54. El-Khoury F, Bignon J, Martin JR. Jouvence, a new human snoRNA involved in the control of cell proliferation. *BMC Genomics* 2020;**21**:817. https://doi.org/10.1186/s12864-020-07197-3
55. McMahon M, Contreras A, Holm M *et al.* A single H/ACA small nucleolar RNA mediates tumor suppression downstream of oncogenic RAS. *eLife* 2019;**8**:e48847. https://doi.org/10.7554/eLife.48847
56. Yoshida K, Toden S, Weng W *et al.* SNOR. *eBioMedicine* 2017;**22**:68–77. https://doi.org/10.1016/j.ebiom.2017.07.009
57. Wang G, Li J, Yao Y *et al.* Small nucleolar RNA 42 promotes the growth of hepatocellular carcinoma through the p53 signaling pathway. *Cell Death Discov* 2021;**7**:347. https://doi.org/10.1038/s41420-021-00740-5

58. Elliott BA, Ho HT, Ranganathan SV *et al.* Modification of messenger RNA by 2'-O-methylation regulates gene expression *in vivo*. *Nat Commun* 2019;**10**:3401. https://doi.org/10.1038/s41467-019-11375-7
59. Adachi H, De Z, Yu YT. Post-transcriptional pseudouridylation in mRNA as well as in some major types of noncoding RNAs. *Biochim Biophys Acta Gene Regul Mech* 2019;**1862**:230–9. https://doi.org/10.1016/j.bbagrm.2018.11.002
60. Kariko K, Muramatsu H, Welsh FA *et al.* Incorporation of pseudouridine into mRNA yields superior nonimmunogenic vector with increased translational capacity and biological stability. *Mol Ther* 2008;**16**:1833–40. https://doi.org/10.1038/mt.2008.200
61. Nakamoto MA, Lovejoy AF, Cygan AM *et al.* mRNA pseudouridylation affects RNA metabolism in the parasite *Toxoplasma gondii*. *RNA* 2017;**23**:1834–49. https://doi.org/10.1261/rna.062794.117
62. Li X, Zhu P, Ma S *et al.* Chemical pulldown reveals dynamic pseudouridylation of the mammalian transcriptome. *Nat Chem Biol* 2015;**11**:592–7. https://doi.org/10.1038/nchembio.1836
63. Anderson BR, Muramatsu H, Nallagatla SR *et al.* Incorporation of pseudouridine into mRNA enhances translation by diminishing PKR activation. *Nucleic Acids Res* 2010;**38**:5884–92. https://doi.org/10.1093/nar/gkq347
64. Hoernes TP, Heimdorfer D, Kostner D *et al.* Eukaryotic translation elongation is modulated by single natural nucleotide derivatives in the coding sequences of mRNAs. *Genes* 2019;**10**:84. https://doi.org/10.3390/genes10020084
65. Eyler DE, Franco MK, Batool Z *et al.* Pseudouridinylation of mRNA coding sequences alters translation. *Proc Natl Acad Sci USA* 2019;**116**:23068–74. https://doi.org/10.1073/pnas.1821754116

Received: July 15, 2024. **Revised:** February 19, 2025. **Editorial Decision:** March 7, 2025. **Accepted:** March 12, 2025